the plant journal

SEB Society for Experimental Biology

The Plant Journal (2017) **89,** 940–956 doi: 10.1111/tpj.13433

Small acidic protein 1 and SCF^{TIR1} ubiquitin proteasome pathway act in concert to induce 2,4-dichlorophenoxyacetic acid-mediated alteration of actin in Arabidopsis roots

Maho Takahashi[1,†], Kana Umetsu[1,†], Yutaka Oono[2], Takumi Higaki[3], Elison B. Blancaflor[4] and Abidur Rahman[1,5,*]

[1]*Cryobiofrontier Research Center, Faculty of Agriculture, Iwate University, Morioka 020-8550, Japan,*

[2]*Department of Radiation-Applied Biology, Quantum Beam Science Research Directorate, National Institutes for Quantum and Radiological Science and Technology (QST), Takasaki 370-1292, Japan,*

[3]*Department of Integrated Biosciences, Graduate School of Frontier Sciences, The University of Tokyo, Kashiwa 277-8562, Japan,*

[4]*Plant Biology Division, The Samuel Roberts Noble Foundation, Ardmore, OK 73401, USA, and*

[5]*Department of Plant Bio Sciences, Faculty of Agriculture, Iwate University, Morioka 020-8550, Japan*

Received 15 June 2016; revised 9 November 2016; accepted 14 November 2016; published online 25 November 2016.

*For correspondence (e-mail abidur@iwate-u.ac.jp).

†These authors contributed equally.

SUMMARY

2,4-Dichlorophenoxyacetic acid (2,4-D), a functional analogue of auxin, is used as an exogenous source of auxin as it evokes physiological responses like the endogenous auxin, indole-3-acetic acid (IAA). Previous molecular analyses of the auxin response pathway revealed that IAA and 2,4-D share a common mode of action to elicit downstream physiological responses. However, recent findings with 2,4-D-specific mutants suggested that 2,4-D and IAA might also use distinct pathways to modulate root growth in Arabidopsis. Using genetic and cellular approaches, we demonstrate that the distinct effects of 2,4-D and IAA on actin filament organization partly dictate the differential responses of roots to these two auxin analogues. 2,4-D but not IAA altered the actin structure in long-term and short-term assays. Analysis of the 2,4-D-specific mutant *aar1-1* revealed that small acidic protein 1 (SMAP1) functions positively to facilitate the 2,4-D-induced depolymerization of actin. The ubiquitin proteasome mutants *tir1-1* and *axr1-12*, which show enhanced resistance to 2,4-D compared with IAA for inhibition of root growth, were also found to have less disrupted actin filament networks after 2,4-D exposure. Consistently, a chemical inhibitor of the ubiquitin proteasome pathway mitigated the disrupting effects of 2,4-D on the organization of actin filaments. Roots of the double mutant *aar1-1 tir1-1* also showed enhanced resistance to 2,4-D-induced inhibition of root growth and actin degradation compared with their respective parental lines. Collectively, these results suggest that the effects of 2,4-D on actin filament organization and root growth are mediated through synergistic interactions between SMAP1 and SCF^{TIR1} ubiquitin proteasome components.

Keywords: Auxin, Actin, Root growth, auxin signaling, SMAP1, ubiquitin proteasome pathway, *Arabidopsis thaliana*.

INTRODUCTION

2,4-Dichlorophenoxyacetic acid (2,4-D), a functional analogue of the endogenous auxin indole-3-acetic acid (IAA), is widely used as a source of auxin as it induces auxin like activities such as inhibition of root growth and induction of lateral roots (Maher and Martindale, 1980). Because of the labile nature of IAA under blue and ultraviolet light (Stasinopoulos and Hangarter, 1990) and the greater stability of 2,4-D in growth media, 2,4-D has been preferred over IAA as an exogenous source of auxin in physiological experiments and forward genetic screens. 2,4-D has been shown to differ from IAA in transport, where it is effluxed more slowly, and in metabolism, where 2,4-D is assumed to accumulate inside the cell to a greater extent because of its slower rate of breakdown (Delbarre *et al.*, 1996; Jackson *et al.*, 2002; Campanoni and Nick, 2005; Staswick *et al.*, 2005). In Arabidopsis, forward genetic screening on 2,4-D largely resulted in the identification of mutants that show altered response to both IAA and 2,4-D (Estelle and

Somerville, 1987), indicating that IAA and 2,4-D share a common mode of action (reviewed in Mockaitis and Estelle, 2008; De Rybel *et al.*, 2009). Functional analyses of several auxin-resistant mutants revealed that auxin signaling is centered on the ubiquitin proteasome pathway-dependent degradation of the transcriptional repressors auxin/IAA (AUX/IAA) (reviewed in Mockaitis and Estelle, 2008). AUX/IAA degradation is directly regulated by SCF$^{TIR1/AFB}$ complex, consisting of S-phase kinase-associated protein 1 (SKP1), CULLIN 1 (CUL1), RING H2 finger 1 (RBX1) and the substrate recognition F-box protein transport inhibitor 1 (TIR1) or its homologues, the auxin signaling F-box (AFB) proteins (Dharmasiri *et al.*, 2005). Auxin directly binds to TIR1/AFB proteins, which promotes the interaction of SCF$^{TIR1/AFB}$ with AUX/IAA proteins, and facilitates ubiquitination with the help of two other enzymes – auxin resistant 1 (AXR1)/E1 C-terminal-related 1 (ECR1) and RUB-conjugating enzyme 1 (RCE1). The ubiquitinated AUX/IAA is degraded by the 26S proteasome, resulting in the release of one or more auxin response factors (ARFs) that regulate auxin-dependent gene expression and hence downstream events (reviewed in Mockaitis and Estelle, 2008). This signaling system has been shown to be a central factor in the plant response to both endogenous and chemically synthesized auxins, including 2,4-D, although with differential sensitivities. 2,4-D shows a 100-fold lower affinity than IAA to bind TIR1 (Kepinski and Leyser, 2005).

Mutant screening against the auxin signaling inhibitor *p*-chlorophenoxyisobutyric acid (PCIB) resulted in isolation of several anti-auxin resistant (*aar*) mutants (*aar1* and *aar3*), which show specific resistance to 2,4-D but wild-type sensitivity to IAA (Rahman *et al.*, 2006; Biswas *et al.*, 2007). Genes encoding small acidic protein 1 (SMAP1) and defective in cullin neddylation-1 (DCN-1)-like protein are the mutated genes in aar1 and *aar3*, respectively (Rahman *et al.*, 2006; Biswas *et al.*, 2007). Physiological and genetic analyses revealed that SMAP1 functions upstream of the AUX/IAA protein degradation pathway and physically interacts with a ubiquitin pathway component, constitutive photomorphogenic9 signalosome (CSN), via the SMAP1 F/D region (Rahman *et al.*, 2006; Nakasone *et al.*, 2012). Genetic analyses further revealed that only under limiting CSN functionality SMAP1 assists plant's response to IAA, but under normal functionality it confers only 2,4-D sensitivity (Nakasone *et al.*, 2012). These findings suggest that a 2,4-D-specific pathway exists in plants. However, the role of this pathway in plant development remains enigmatic.

Exogenous application of IAA or 2,4-D typically results in inhibition of root growth (Maher and Martindale, 1980). Although for a long time it was believed that IAA and 2,4-D inhibit root growth through similar mechanisms, we previously showed that IAA and 2,4-D use both overlapping and distinct pathways to regulate the root growth process. At a concentration of IAA and 2,4-D that inhibits root growth around 50%, IAA solely affects cell elongation, while 2,4-D largely affects cell division (Rahman *et al.*, 2007). Interestingly, 2,4-D and IAA exert opposite effects in altering the cytoskeletal structure of root cells. While 2,4-D degrades actin, IAA induces bundling (Rahman *et al.*, 2007). The bona fide actin inhibitor latrunculin B (Lat B) mimicked the effects of 2,4-D on cell division and cell elongation during root growth, suggesting that the disruption of actin caused by 2,4-D might account for its inhibitory effect on cell division. The isolation of 2,4-D-specific root growth mutants, and the distinct mechanistic difference between IAA and 2,4-D in modulating root growth, confirm that the native and synthetic auxins have mechanistically distinct, but partially overlapping, pathways. Collectively, these results reveal SMAP1 and actin to be two major components for modulating 2,4-D response. However, the questions that remain unanswered are: is root growth resistance to 2,4-D in *aar1* linked to the cellular actin status and does SMAP1 have any functional role in controlling 2,4-D-mediated actin degradation?

In the present work, we demonstrate that: (i) actin plays a central role in eliciting the 2,4-D response in roots, and (ii) SMAP1 and the ubiquitin proteasome pathway act synergistically and function as positive modulators for 2,4-D-induced alteration of actin in roots.

RESULTS

The response of primary root growth to 2,4-D relies on intracellular actin organization

To understand the specificity 2,4-D action, we investigated its effect on primary root growth and actin organization in the auxin influx mutant *aux1-7* (Bennett *et al.*, 1996). *AUX1* encodes an amino acid permease-like uptake carrier, which functions in facilitating the uptake of endogenous auxin IAA, and its functional analogue 2,4-D with high affinity (Carrier *et al.*, 2008). Absence of AUX1 results in approximately 50% reduction in IAA or 2,4-D uptake (Marchant *et al.*, 1999; Rahman *et al.*, 2001a). In root growth assays, *aux1-7* shows resistance to both IAA and 2,4-D but wild-type sensitivity to NAA, and application of exogenous NAA rescues the gravity defect of *aux1* (Maher and Martindale, 1980; Yamamoto and Yamamoto, 1998; Marchant *et al.*, 1999; Rahman *et al.*, 2001b). Consistent with earlier reports, we found that *aux1-7* showed a strong resistance to the growth-inhibiting effects of 2,4-D on root elongation. The relatively high concentration of 2,4-D (100 nM) which almost completely inhibited the root elongation in wild-type seedlings had barely any effect on root elongation of *aux1-7* (Figure 1A), confirming that 2,4-D uptake is severely perturbed in this mutant.

2,4-D has been shown to affect root elongation by modulating the actin cytoskeletal structure (Rahman *et al.*,

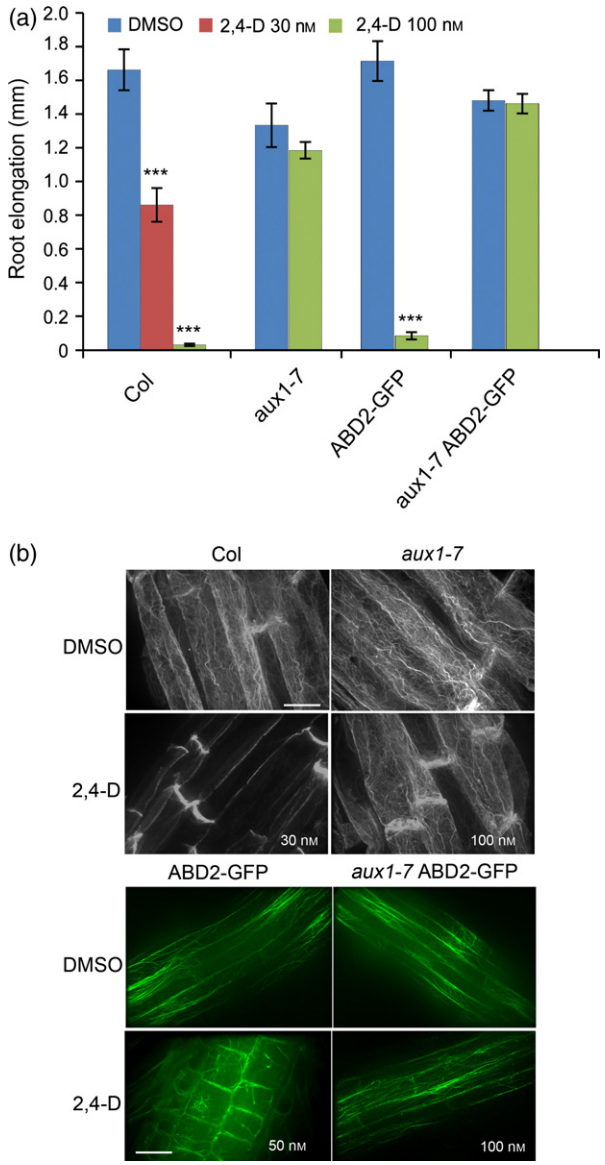

Figure 1. Auxin uptake mutant *aux1-7* shows strong resistance to 2,4-dichlorophenoxyacetic acid (2,4-D)-induced root growth inhibition and actin alteration.

(a) Effect of 2,4-D on root elongation. Five-day old Arabidopsis seedlings were transferred to new agar plates and subjected to 2,4-D treatment for 48 h. Vertical bars represent mean ± SE of the experimental means from at least four independent experiments ($n = 4$ or more), where experimental means were obtained from 8–10 seedlings per experiment. Asterisks represent the statistical significance between control and treatment as judged by the Student's *t*-test ($P < 0.0001$).

(b) Effects of 2,4-D on intracellular actin organization of wild type and *aux1-7*. Upper panel, chemical fixation; lower panel, live cell imaging. The images are representative of at least three independent experiments, with six to eight roots per treatment in each run. The figure shows epidermal cells from the maturation zone. Five-day old Arabidopsis seedlings were transferred to new agar plates and subjected to 2,4-D treatment for 48 h. After the treatment, roots were fixed (for chemical fixation) or mounted in liquid growth medium on a cover glass (for live cell imaging) and actin was localized using confocal laser scanning microscopy. Note that images were taken from the same area. The changes in the cell shape in ABD2-GFP is due to the high concentration of 2,4-D. Images are projections of 10–12 optical sections. Bars represent 10 μm.

2007), which prompted us to investigate the effect of 2,4-D in regulating actin arrangement in *aux1-7*. To visualize actin, we used immunocytochemistry and live cell imaging. For immunostaining, roots were chemically fixed followed by staining with an anti-actin antibody (Rahman *et al.*, 2007); for live cell imaging, we used a transgenic line expressing a GFP-fusion to the actin-binding domain 2 from fimbrin (ABD2-GFP) (Wang *et al.*, 2004; Rahman *et al.*, 2007). Wild-type plants expressing ABD2-GFP were crossed with *aux1-7* to obtain *aux1-7*ABD2-GFP. In root elongation assays, wild-type lines expressing ABD2-GFP and *aux1-7*ABD2-GFP showed similar sensitivity and resistance as the wild type and *aux1-7*, respectively, in presence of 2,4-D (Figure 1A). In DMSO-treated wild-type and *aux1-7* roots, typical long filamentous actin was observed in the elongating cells in both immunostained samples (Figure 1B, upper panel) and live cells (Figure 1B, lower panel). Consistent with previous results, 30 nM 2,4-D disrupted the organization of actin filaments, accompanied by an increased fluorescence signal at the end walls (Figure 1B). In wild-type background, 30 nM 2,4-D was the upper limit for immunostaining as treatment with higher concentrations of 2,4-D resulted in an abundance of long root hairs, which made binding of antibody to the epidermal cells irregular and difficult. In contrast, in *aux1* or *aux1-7*ABD2-GFP roots, actin organization was not affected even at 100 nM 2,4-D (Figure 1B). The *aux1* mutant also showed a strong resistance to 2,4-D-induced inhibition of root growth at 100 nM (Figure 1A). Consistently, 2,4-D-induced changes in cell expansion and shape were absent in the *aux1-7* background (Figure 1B). Taken together, these results suggest that the observed changes in cell shape and root growth resulting from 2,4-D treatment in wild type are linked to intracellular actin organization.

2,4-D but not IAA promotes the depolymerization of actin filament

To confirm the link between 2,4-D and actin, and distinguish the difference between the effect of IAA and 2,4-D on actin, we quantified actin filament organization in wild-type seedlings expressing ABD2-GFP using metrics developed by Higaki *et al.* (2010). Actin was quantified after the seedlings were treated with 1 and 3 μM IAA or 2,4-D for 1 h (Figure 2). The short incubation of 1 h was used to rule out the possibility of rapid conversion of IAA to 2-oxoindole-3-acetic acid (oxIAA), and two different concentrations were used to assess the potency of 2,4-D and IAA. A feeding experiment using [$^{13}C_6$]-IAA in Arabidopsis seedlings revealed that a detectable increase in oxIAA and oxIAA-glucoside could be observed only after 3 h of treatment (Porco *et al.*, 2016), confirming that the degradation of IAA is minimal in this experimental setup. Four different parameters were obtained for actin quantification: occupancy, skewness, $\Delta\theta$ and NormAvgRad (Higaki *et al.*, 2010;

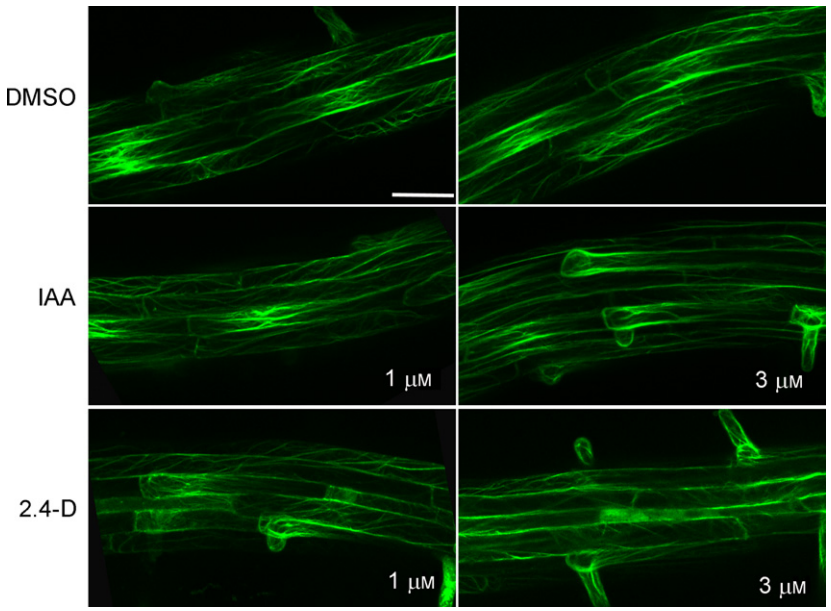

Figure 2. Effect of 2,4-dichlorophenoxyacetic acid (2,4-D) and indole-3-acetic acid (IAA) on cellular actin organization during short time incubation.
The images are representative of at least three independent experiments, with five to six roots per treatment in each run. Shown are epidermal cells from the maturation zone. Five-day-old ABD2-GFP seedling were transferred to a six-well Petri dish containing liquid Hoagland growth medium supplemented with or without 1 μM and 3 μM IAA or 2,4-D and incubated for 1 h. After the incubation, roots were mounted in liquid growth medium on a cover glass and actin was imaged with confocal laser scanning microscopy using the same laser settings. Images are projections of eight optical sections. Bars represent 50 μm.

Ueda *et al.*, 2010). Occupancy represents a metric for density, skewness for bundling, $\Delta\theta$ for orientation and NormAvgRad for parallelness of the actin filaments (see Experimental Procedures for definitions). Under our conditions, there were no measurable differences in actin filament organization between IAA- and 2,4-D-treated roots with regard to orientation and NormAvgRad. However, density and bundling of actin filaments were significantly lower in 2,4-D-treated roots when compared with untreated and IAA-treated roots (Figure 3). Previous studies demonstrated that occupancy reflects the extent of microfilament depolymerization and is sensitive to the actin polymerization inhibitor Lat B (Higaki *et al.*, 2010). Skewness, the metric for bundling, has also been shown to be altered by the actin stabilizer jasplakinolide and villins (Higaki *et al.*, 2010; Khurana *et al.*, 2010).The selective reduction of density and the bundling of the actin filaments after short-term treatment with 2,4-D suggests that 2,4-D has a rapid effect on actin filament organization, and likely exerts its effect on actin structure through depolymerization.

aar1 is resistant to 2,4-D-induced actin depolymerization

To further understand the role of actin in regulating the 2,4-D response, we next used *aar1-1*, a mutant that shows specific resistance to 2,4-D-induced root growth inhibition (Rahman *et al.*, 2006). *AAR1* encodes SMAP1 and functions upstream of the auxin signaling pathway (Rahman *et al.*, 2006; Nakasone *et al.*, 2012). Because 2,4-D but not IAA degrades actin (Rahman *et al.*, 2007), we hypothesized that the specific resistance of *aar1-1* to 2,4-D may be linked to cellular actin organization, and in the absence of SMAP1, 2,4-D is unable to depolymerize actin.

To test the above hypothesis, we first investigated the effect of 2,4-D on intracellular actin organization using both live cell imaging and chemical fixation. In contrast to the effect observed in wild type, 30 nM 2,4-D did not alter actin organization in the loss of *SMAP1* background lines *aar1* and 520i 1G (a RNAi silencing line of SMAP1; Rahman *et al.*, 2006) (compare Figures 1B and 4). In immunostained samples, long filamentous actin, comparable to the control treatment, was visible in the presence of 30 nM 2,4-D in both *aar1* and 520i 1G (Figure 4, upper panel). Similar results were observed in live cells using homozygous *aar1* ABD2-GFP transgenic lines (Figure 6, lower panel), confirming that SMAP1 links actin to 2,4-D response.

Next, we focused on root growth analysis and performed physiological and cellular characterization of *aar1-1* and 520i 1G using a long-term assay. In this assay, we used yellow light conditions to prevent the degradation of IAA. The effect of IAA on root growth under yellow light condition is significantly different from that under white light condition, and showed a similar dose response pattern like 2,4-D for root growth inhibition (Rahman *et al.*, 2001b, 2007). The root growth assay in IAA and 2,4-D confirmed the previous observation that loss of *SMAP1* confers specific resistance to 2,4-D, while the mutants show wild-type sensitivity to IAA (Figure 5, Rahman *et al.*, 2006). Compared with the type, *aar1* and 520i 1G roots showed an increased resistance to 2,4-D. In wild type, 30 nM 2,4-D resulted in approximately 50% inhibition of root elongation, while 50 nM 2,4-D was required to achieve similar inhibition in *aar1-1* and 520i 1G (Figure 5). Consistently, at 30 nM 2,4-D, *aar1* and 520i 1G showed strong resistance to 2,4-D-induced inhibition of root growth (Figure 5). With increasing concentration of 2,4-D, both the intracellular actin organization and the root elongation of *aar1* and 520i 1G become susceptible to 2,4-D. Treatment with 50 nM 2,4-D showed decreasing actin signals in *aar1*, 520i 1G and

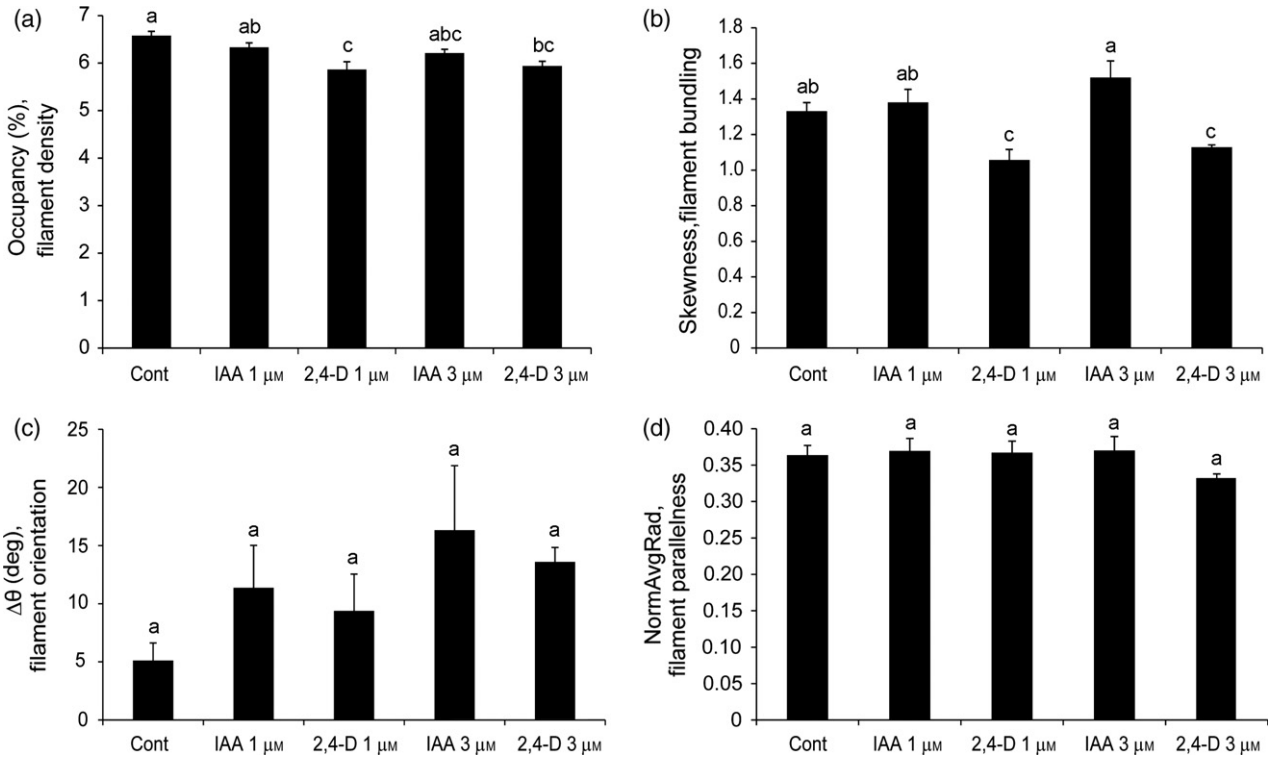

Figure 3. Quantification of actin filaments.
Effect of short-term incubation with 2,4-dichlorophenoxyacetic acid (2,4-D) and indole-3-acetic acid (IAA) on various parameters of actin filaments. Cells obtained from the images in Figure 2 were subjected to actin quantification as described earlier by Higaki *et al.* (2010).
(a) Percent occupancy, which reflects the filament density.
(b) Skewness, which reflects the bundling of the actin filaments.
(c) $\Delta\theta$ (degrees), which reflects the filament orientation.
(d) NormAvgRad, which reflects the parallelness of the filaments.
Vertical bars represent mean ± SE of the experimental means from at least three independent experiments ($n = 3$ or more), where experimental means were obtained from 30–40 cells. Comparisons between multiple groups were performed by analysis of variance (ANOVA) followed by the Tukey–Kramer test. The same letter indicates that there are no significant differences ($P < 0.05$).

aar1 ABD2-GFP roots (Figure 4), although remnants of fine filamentous actin could still be observed (Figure 4). Consistently, 50 nM 2,4-D treatment did not affect cell morphology in the *aar1* background, although it induced severe changes in the wild-type background (compare Figures 1B and 4). These results indicate that the alteration of cell morphology depends on the extent of actin filament depolymerization. To further confirm that the effect of 2,4-D is not allele dependent, we performed the root growth assay in two *aar1* complemented lines, B/S1G, B/S2D, and a non-complemented line, X/B, as described earlier (Rahman *et al.*, 2006). In the complemented lines, the response of root elongation to 2,4-D was completely recovered, while the non-complemented line showed resistance (Figure S1 in the Supporting Information). Taken together, our results show that the specific resistance of *aar1* or RNA silencing line 520i 1G to 2,4-D-induced inhibition of root growth is due in part to an actin cytoskeleton that is less susceptible to 2,4-D-triggered depolymerization.

SMAP1 acts as a positive regulator for 2,4-D-induced inhibition of cell division and cell elongation

Root growth rate is regulated by the combined activity of two linked processes, cell expansion and cell production (Beemster and Baskin, 1998). Earlier it was reported that the endogenous auxin IAA and its functional analogue 2,4-D evoke differential responses in regulating root growth; 2,4-D mainly affects cell division, while IAA affects cell elongation (Rahman *et al.*, 2007). Because 2,4-D but not IAA alters actin filament organization, and the actin depolymerizing drug Lat B mimics the effect of 2,4-D on cell division, it was hypothesized that the differential response of cell division to IAA and 2,4-D is linked to the differential effect of these two auxins on the actin cytoskeleton (Rahman *et al.*, 2007). Since loss of SMAP1 attenuates the effect of 2,4-D on cellular actin structure, we next explored how SMAP1 integrates cell division, cell elongation and actin.

To evaluate the role of SMAP1 on 2,4-D-induced inhibition of cell division and cell elongation, we took a kinematic

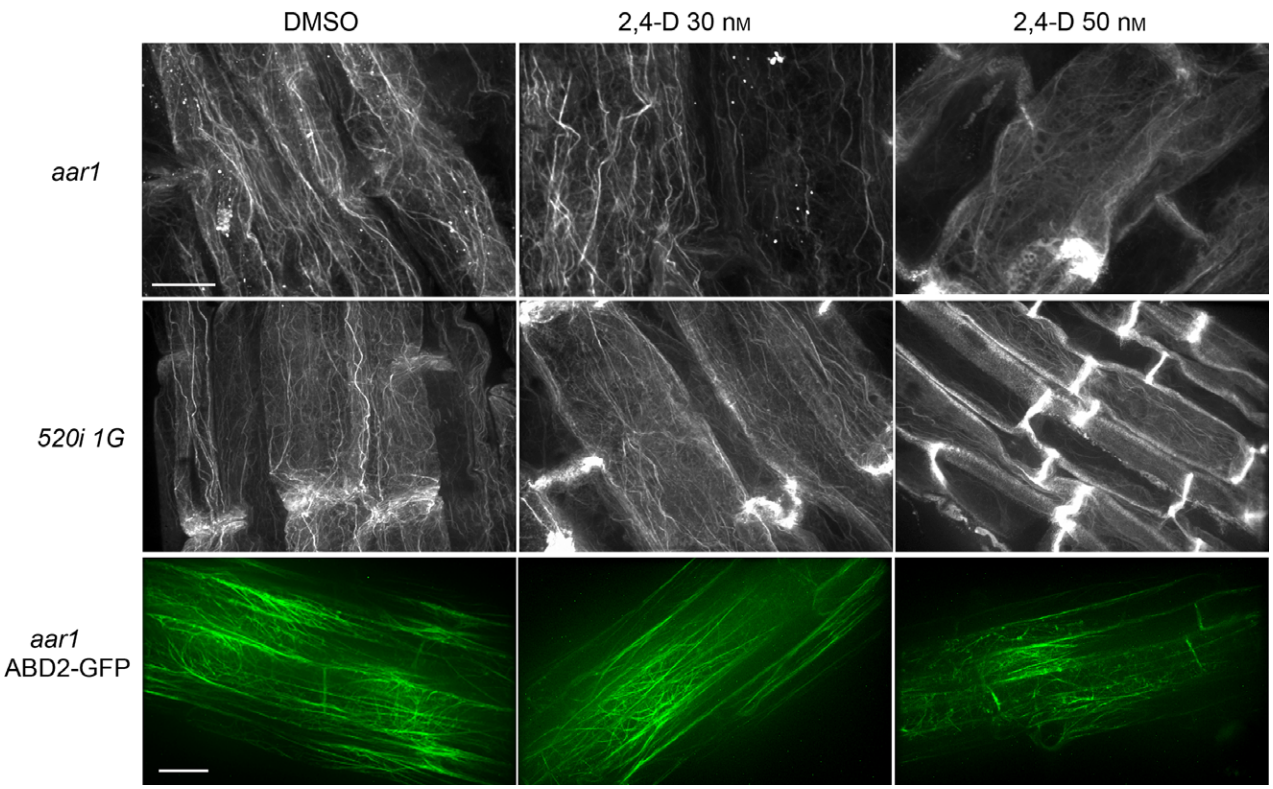

Figure 4. *aar1* mutant shows resistance to 2,4-dichlorophenoxyacetic acid (2,4-D)-induced alteration of actin structure.
Effects of 2,4-D on intracellular actin organization of *aar1*-1 and a RNA line of SMAP1, 520i 1G. Upper panel, chemical fixation; lower panel, live cell imaging. The images are representative of at least three independent experiments, with six to eight roots per treatment in each run. The figure shows epidermal cells from the maturation zone. Five-day-old Arabidopsis seedlings were transferred to new agar plates and subjected to 2,4-D treatment for 48 h. After the treatment, roots were fixed (for chemical fixation) or mounted in liquid growth medium on a cover glass (for live cell imaging), and actin was localized using confocal laser scanning microscopy. Images are projections of 10–12 optical sections. Bars represent 10 μm.

approach as described previously (Rahman *et al.*, 2007). The root elongation rate and the length of newly matured cortical cells were measured in the wild type, *aar1-1* and RNAi silencing lines of SMAP1 (520i 1G and 520i 2C). The ratio of mature cell length to root elongation rate gives the time required to produce one cortical cell (per cell file), which is also defined as the cell production rate (Silk *et al.*, 1989). This cell production rate represents the output of the meristem, reflecting both the number of dividing cells and their rates of division. For cell production assay, two concentrations of 2,4-D were used. One was a low concentration of 2,4-D (30 nM), which induces approximately 50% inhibition in wild-type root growth, and the other was a relatively high concentration (50 nM), which severely inhibits root elongation in the wild type (Table 1). *aar1-1* and RNAi silencing lines showed complete resistance to 30 nM 2,4-D and could elongate approximately 50% on 50 nM 2,4-D (Table 1).

Consistent with previous data, we found that 30 nM 2,4-D largely affected cell division, which explains its inhibitory effect on root elongation in wild type (Table 1; Rahman *et al.*, 2007). In contrast, a higher concentration of 2,4-D (50 nM) drastically reduced the cell length in wild type (Table 1). Due to the extreme reduction of the elongation rate, it was difficult to calculate the cell production rate. On the other hand, *aar1-1* and the RNAi silencing lines showed complete resistance to 30 nM 2,4-D-induced inhibition of root growth. In these lines, neither cell length nor the cell production rate were affected (Table 1). The reduction in the root elongation of *aar1-1* and RNAi silencing lines at a higher concentration of 2,4-D was attributed solely to the reduction in cell division; cell elongation showed complete resistance to this treatment (Table 1).

The resistance of the loss of SMAP1 mutants towards 2,4-D-induced depolymerization of actin, as well as inhibition of cell division and cell elongation, provides genetic evidence that SMAP1 acts as a positive regulator for 2,4-D in modulating these processes.

The ubiquitin proteasome pathway functions in 2,4-D-induced degradation of actin filaments

The ubiquitin proteasome pathway plays a central role in regulating auxin signaling. TIR1, a component of E3 ligase, with the help of two other ubiquitin-activating and -conjugating enzymes E1 and E2, promotes the degradation of AUX/IAA proteins that block auxin-responsive gene

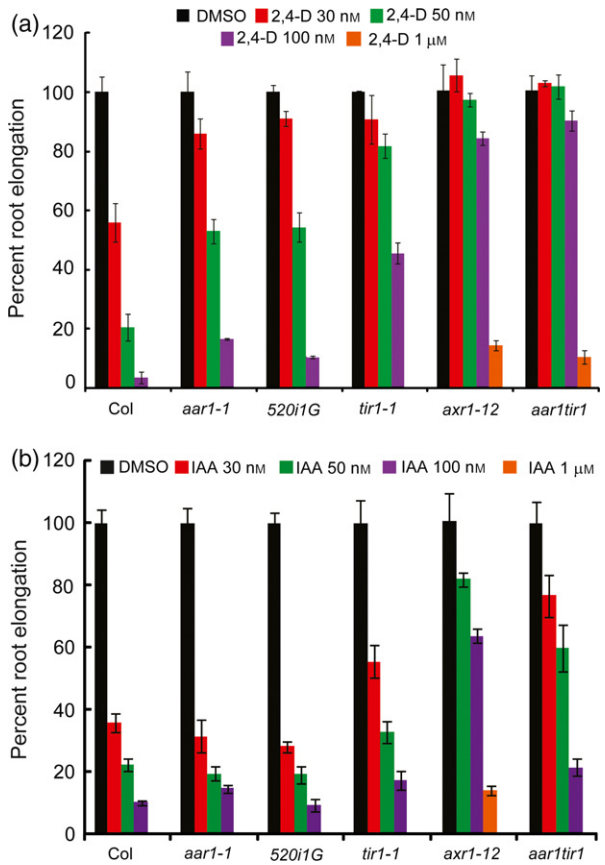

Figure 5. Comparison of the effect of 2,4-dichlorophenoxyacetic acid (2,4-D) and indole-3-acetic acid (IAA) on root growth inhibition in various auxin-related mutants.
(a) Effect of 2,4-D on root elongation.
(b) Effect of IAA on root elongation.
Five-day old Arabidopsis seedlings were transferred to new agar plates and subjected to 2,4-D or IAA treatment for 48 h. Vertical bars represent mean ± SE of the experimental means from at least four independent experiments (n = 4 or more), where experimental means were obtained from 8–10 seedlings per experiment.

expression by repressing auxin response factor (ARF) (Leyser, 2002). The response of root growth to 2,4-D has also been shown to be regulated by this pathway, as mutants belonging to the ubiquitin response pathway show resistance to both IAA and 2,4-D (Estelle and Somerville, 1987). Since 2,4-D-induced inhibition of root growth is linked to cellular actin organization, we assumed that the resistance of ubiquitin-related mutants to 2,4-D may involve both the auxin signaling pathway and actin. To clarify the relationship between the ubiquitin response pathway and 2,4-D-mediated modification of actin, we characterized auxin receptor mutants and a mutant that is strongly deficient in ubiquitin-mediated auxin signaling. Arabidopsis has several TIR1-like receptor proteins. Phylogenetic studies suggested that TIR1/AFB proteins are conserved in land plants and they can be divided into three distinct lineages, namely TIR1/AFB2, AFB4 and AFB6 (Parry *et al.*, 2009). Arabidopsis does not have any AFB6 homologue. AFB5, which belongs to the AFB4 lineage, has been shown to function as receptor for synthetic picolinate auxins but not for IAA or 2,4-D (Walsh *et al.*, 2006; Gleason *et al.*, 2011). Among other AFBs, TIR1 and AFB2 have been shown to play a major role in regulating auxin response (Dharmasiri *et al.*, 2005). Hence, in our analysis, we selected *tir1-1* and *afb2-1* mutants as representative auxin receptor mutants. Because of the presence of several receptor complexes, the receptor mutants are in general phenotypically weak mutants (Dharmasiri *et al.*, 2005). As a representative of strong auxin signaling mutant, we used *axr1*, where *AXR1* encodes a protein similar to E1 and functions at the very first step of the neddylation process (Leyser *et al.*, 1993; del Pozo and Estelle, 1999; Mockaitis and Estelle, 2008).

Root elongation assay of *tir1*, *afb2* and *axr1* against IAA and 2,4-D revealed that all these mutants consistently showed more resistance to 2,4-D compared with IAA at all

Table 1 Effect of 2,4-dichlorophenoxyacetic acid (2,4-D) on cell length and cell production rate

	Treatment	Primary root elongation (mm day^{-1})	Cell length (mm)	Cell production rate (cells day^{-1})
Col	DMSO	9.7 ± 0.2 (100)	184 ± 9.2 (100)	50.6 ± 0.9 (100)
	2,4-D 30 nM	5 ± 0.4 (52)	174 ± 0.6 (95)	28.9 ± 2.5 (57)
	2,4-D 50 nM	0.5 ± 0.3 (5)	15 ± 5.7 (8)	N/A
aar1-1	DMSO	7.9 ± 0.4 (100)	178 ± 6.0 (100)	44.3 ± 1.4 (100)
	2,4-D 30 nM	7.6 ± 0.1 (96)	190 ± 8.2 (107)	40.0 ± 1.2 (90)
	2,4-D 50 nM	4.2 ± 0.4 (53)	182 ± 2.3 (102)	22.9 ± 2.0 (52)
520i 1G	DMSO	9.8 ± 0.4 (100)	197 ± 6.7 (100)	50.0 ± 1.0 (100)
	2,4-D 30 nM	9 ± 0.3 (92)	189 ± 10.7 (96)	48.0 ± 4.4 (96)
	2,4-D 50 nM	5.1 ± 0.7 (52)	169 ± 2.3 (86)	30.6 ± 4.7 (61)
520i 2C	DMSO	9.5 ± 0.06 (100)	185 ± 7.6 (100)	51.5 ± 2.5 (100)
	2,4-D 30 nM	8.3 ± 0.3 (87)	197 ± 8.0 (107)	42.0 ± 0.1 (82)
	2,4-D 50 nM	4.5 ± 0.3 (47)	171 ± 9.2 (93)	26.5 ± 3.2 (51)

Data are means ± SEM of three replicate experiments. Values in parentheses are the percentage of control value for each column.

concentrations tested (Figures 5 and S2). Additionally, to rule out the possibility of an allele-specific effect of 2,4-D on *tir1*, we used another T-DNA insertion allele, *tir1-10*. Consistent with *tir1-1*, *tir1-10* also showed increased resistance to 2,4-D compared with IAA for root growth inhibition (Figure S1). The strong resistance of auxin receptor mutants, irrespective of their lineages and alleles, to 2,4-D over IAA suggests that the differential response of these mutants cannot possibly be explained by selective affinities of the various receptor complexes toward IAA and 2,4-D (Calderón Villalobos *et al.*, 2012). However, we do not completely rule out this possibility as there are various combinations of AFB–AUX/IAA that may change the affinity of the receptor complexes towards different chemical forms of auxin.

axr1, in which ubiquitin-mediated auxin signaling is abolished, in general showed stronger resistance to both IAA and 2,4-D compared with the receptor mutants for root growth inhibition (Figure 5). Interestingly, this mutant also showed stronger resistance to 2,4-D compared with IAA (Figure 5). Collectively, these results indicate that in addition to the auxin signaling pathway, some additional factors are specifically involved in 2,4-D but not IAA response pathway. To understand whether intracellular actin is the missing factor in contributing to the enhanced resistance of auxin-related ubiquitin mutants to 2,4-D, we imaged actin in *tir1* and *axr1* mutants using both immunostaining and live cell imaging. In *tir1-1*, both approaches revealed that 50 nM 2,4-D failed to alter the actin filament structure, while at 100 nM actin started to break down (Figure 6). The response of the intracellular actin structure to 2,4-D in *tir1-1* paralleled the root elongation response of this mutant to 2,4-D, and was very similar to the results observed in *aar1-1* mutants (Figures 4–6). Consistent with the strong root growth resistance phenotype in 2,4-D, actin in *axr1-12* also showed an enhanced resistance to 2,4-D-induced depolymerization; actin structure remained intact even at 100 nM 2,4-D (Figure 6). *axr1-12* shows very strong flowering and silique phenotypes and as such is not a good subject for crossing. Hence, *axr1-3*, which is a weak allele (Lincoln *et al.*, 1990; Leyser *et al.*, 1993), was crossed with ABD2-GFP. Live cell imaging of actin filaments in roots of *axr1-3* ABD2-GFP showed a similar resistance pattern to that of roots processed by immunostaining (Figure 6). Actin structure was disrupted in both the mutants at a 2,4-D concentration which severely inhibited root growth (1 μM). Taken together, these results confirm that the SCF^{TIR1} ubiquitin proteasome pathway plays an important role in modulating 2,4-D-mediated depolymerization of actin.

Ubiquitin proteasome inhibitor MG132 blocks the effect of 2,4-D on actin

In the long-term root elongation assay, the mutants in the SCF^{TIR1} ubiquitin proteasome pathway show strong resistance to 2,4-D-induced depolymerization of actin, which implies that this pathway possibly regulates the actin response to 2,4-D. However, one potential drawback of the long-term assay is its specificity, as other off- target machineries can also be affected. To clarify the specificity of the ubiquitin pathway in regulating 2,4-D-induced depolymerization of actin, we performed a short-term assay to visualize and quantify the effect of 2,4-D on actin in presence of the general ubiquitin proteasome inhibitor MG132 (Gray *et al.*, 2001). In several studies, treatment with 50 μM MG132 has been shown to successfully block the auxin signaling pathway (Hayashi *et al.*, 2003; Brunoud *et al.*, 2012). In our assay, pre-treatment with 50 μM MG132 for 30 min did not induce any significant changes in actin structure as observed by imaging and quantification (Figure 7). Treatment with 3 μM 2,4-D for 1 h reduced the actin filament density and bundling. However, when the roots pre-treated with MG132 were exposed to 2,4-D, no measurable changes in actin structure were detected (Figure 7). Quantification revealed that MG132 completely blocked the effect of 2,4-D on actin filament organization (Figure 7), confirming that the ubiquitin proteasome pathway modulates the 2,4-D actin pathway.

SMAP1 genetically interacts with SCF^{TIR1} ubiquitin pathway to modulate the response of actin to 2,4-D

Both the *aar1-1* and auxin-related ubiquitin pathway mutants showed increased resistance to 2,4-D-induced actin degradation and root growth inhibition. Interestingly, *aar1-1* showed specific resistance to 2,4-D but not IAA, while the ubiquitin pathway mutants *tir1-1* and *axr1* showed resistance to both IAA and 2,4-D, albeit with different sensitivities (Figure 5). These results raised the possibility that SMAP1 may work independently of the ubiquitin pathway to regulate the action of 2,4-D on intracellular actin. To test this hypothesis, auxin sensitivity of the *aar1-1 tir1-1* double mutant was analyzed. Compared with the respective single-mutant lines, *aar1-1 tir1-1* showed enhanced resistance to 2,4-D-induced inhibition of root growth. For instance, 100 nM 2,4-D, which inhibited approximately 50% and 80% of root growth in *tir1-1* and *aar1-1* single mutants, respectively, only inhibited 20% of root growth in the double mutant (Figure 5). In contrast, at 100 nM IAA, *aar1-1tir1-1* double mutant roots show *tir1-1*-like sensitivity, although at lower concentrations an increased resistance to IAA was observed (Figure 5). Consistently, actin filaments remained intact even with 100 nM 2,4-D treatment in *aar1-1 tir1-1* (Figure 6). As in *axr1*, increased concentration of 2,4-D (1 μM) altered actin structure and drastically inhibited root growth in *aar1 tir1* (Figure 7). Collectively, these results confirm that SMAP1 is specifically involved in 2,4-D-mediated pathways and acts synergistically with the SCF^{TIR1} ubiquitin pathway.

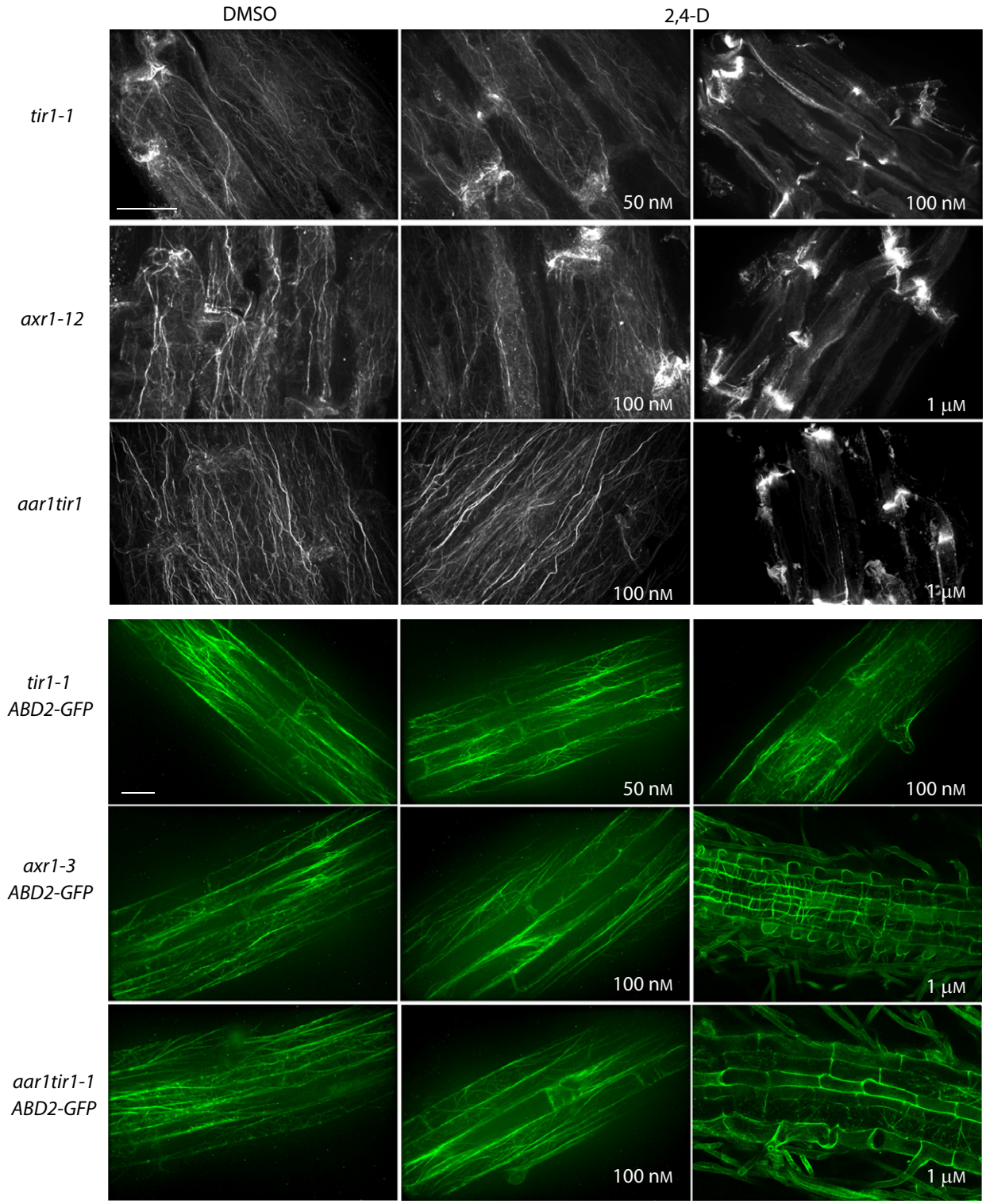

Figure 6. Auxin signaling mutants show strong resistance to 2,4-dichlorophenoxyacetic acid (2,4-D)-induced alteration of actin structure.
Effects of 2,4-D on the intracellular actin organization of *tir1-1*, axr1 and *aar1tir1*. Upper panel, chemical fixation; lower panel, live cell imaging. The images are representative of at least three independent experiments, with six to eight roots per treatment in each run. The figure shows epidermal cells from the maturation zone. Note that the altered cell shape in some images is due to high concentrations of 2,4-D. Five-day-old Arabidopsis seedlings were transferred to new agar plates and subjected to 2,4-D treatment for 48 h. After the treatment, roots were fixed (for chemical fixation) or mounted in liquid growth medium on a cover glass (for live cell imaging) and actin was visualized with confocal laser scanning microscopy using same laser settings. Images are projections of 10–12 optical sections. Bars represent 10 μm.

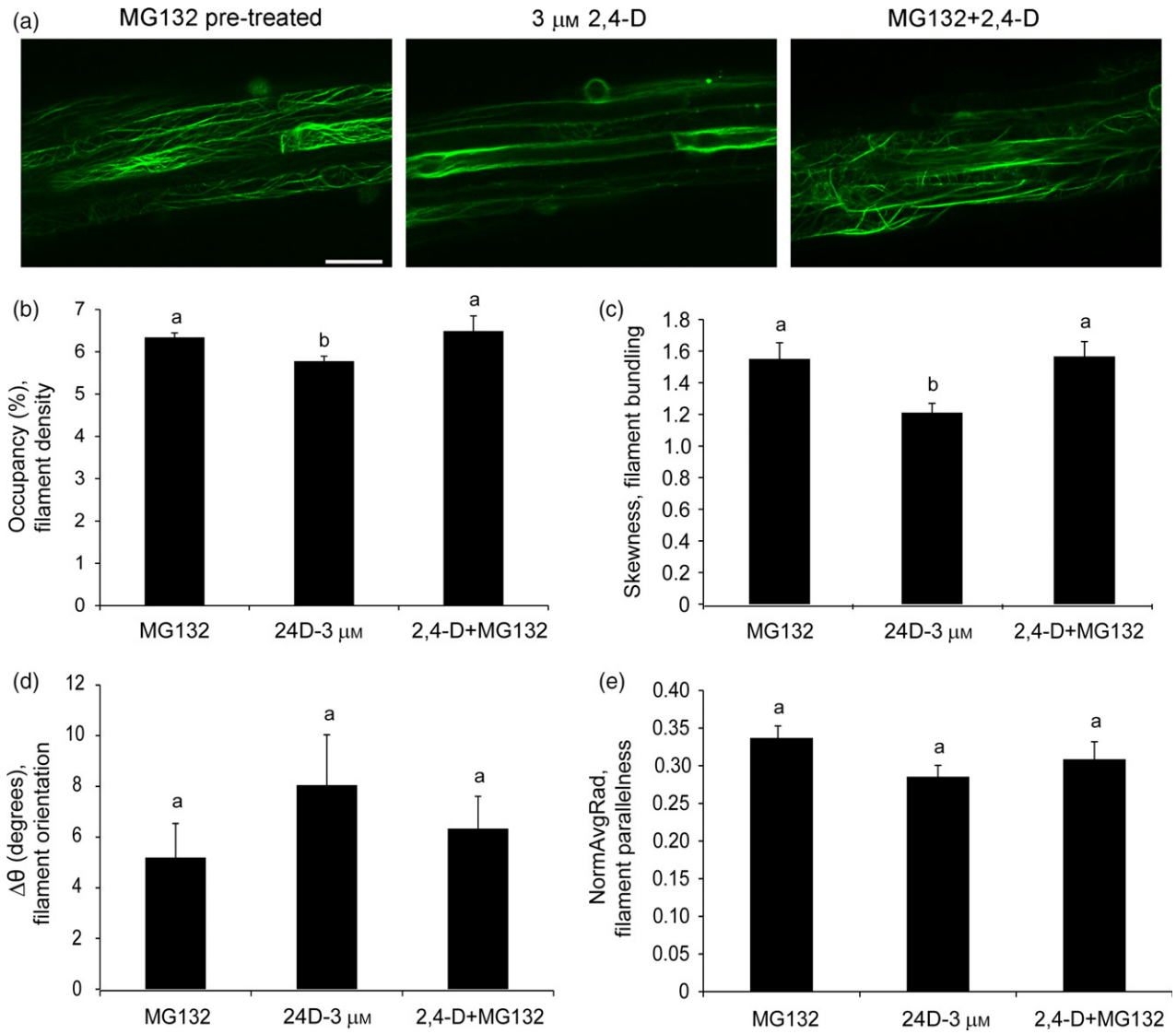

Figure 7. Ubiquitin proteasome inhibitor blocks the 2,4-dichlorophenoxyacetic acid (2,4-D)-induced depolymerization of actin.
Effect of ubiquitin proteasome inhibitor MG132 pretreatment on 2,4-D induced depolymerization of actin.
(a) Representative images of roots of ABD2-GFP seedlings obtained from four independent experiments. Five-day-old ABD2-GFP seedlings were transferred to liquid growth medium and treated with or without 50 μM MG132 for 30 min followed by a treatment with or without 3 μM 2,4-D for 3 h. After the incubation, the actin was visualized with confocal laser scanning microscopy using the same laser settings. Images are projections of eight optical sections. Bars represent 10 μm.
(b) Quantification of actin microfilaments. The quantification was performed exactly as described in the caption to Figure 3. Note that MG132 pre-treatment blocks the 2,4-D-induced reduction in occupancy and skewness. Vertical bars represent mean ± SE of the experimental means from at least three independent experiments (n = 3 or more), where experimental means were obtained from 30–40 cells. Comparisons between multiple groups were performed by analysis of variance (ANOVA) followed by the Tukey–Kramer test. The same letter above the columns indicates that there are no significant differences ($P < 0.05$).

SMAP1 and ubiquitin components are not required for Lat B-induced degradation of actin

Earlier it was reported that Lat B, a bona fide actin inhibitor (Spector *et al.*, 1983, 1989; Coué *et al.*, 1987) affected cell elongation and division similarly to 2,4-D, leading to the hypothesis that disruption of actin caused by 2,4-D is sufficient to account for its effect on cell production and hence on root growth (Rahman *et al.*, 2007). To evaluate whether Lat B also requires SCF^{TIR1} ubiquitin pathway or SMAP1 to inhibit actin polymerization, we investigated the sensitivity of the primary root elongation and actin organization of *aar1* and *tir1* mutants to Lat B. Unlike with 2,4-D, none of the mutants showed resistance to Lat B-induced inhibition of root growth (Figure S3A). Consistently, at a concentration where 50% inhibition of root growth can be achieved, *aar1* and *tir1* showed a wild-type-like sensitivity to Lat B-induced depolymerization of actin, while both the mutants showed clear resistance to 2,4-D-induced degradation of

actin (Figure S3B). These results indicate that SMAP1 and ubiquitin components appear to be essential for 2,4-D- but not for Lat B-induced degradation of actin.

Actin mutants show increased resistance to 2,4-D- but not IAA-induced inhibition of root growth

To further clarify the role of actin in 2,4-D response, we next investigated the response of actin mutants to 2,4-D and IAA. Arabidopsis has two distinct classes of actin, namely vegetative and reproductive. Eight actin isovariants are grouped into these two classes (Kandasamy *et al.*, 2009; Figure S4). Several lines of evidence strongly suggest that the two major classes of plant actin isovariants are functionally distinct. The vegetative actin isovariants expressed in young tissues play a role in meristem development, while plant reproduction is regulated by reproductive actins (Gilliland *et al.*, 2002). Vegetative actin is further divided in two distinct subclasses, subclass 1 containing ACT2 and ACT8 and subclass 2 containing ACT7 (Figure S4). These actin isovariants play distinct subclass-specific roles during plant morphogenesis (Gilliland *et al.*, 2003; Kandasamy *et al.*, 2009). For instance, ACT7 was found to be involved in regulating root growth, epidermal cell specification and root architecture, while ACT2 and ACT8 were essential for root hair tip growth. Since vegetative actin has been shown to play an important role in root development, we used one representative actin mutant from each subclass, *act7-4* and *act2-1*, and investigated their root growth response in presence of IAA and 2,4-D. In these mutants, the levels of respective isovariants of actin are significantly reduced, which resulted in altered seedling phenotype (Kandasamy *et al.*, 2009; Figure S5). The root growth assay results revealed that both *act7* and *act2* showed increased resistance to 2,4-D-induced inhibition of root growth, while they responded to IAA like wild-type (Figures 8 and S5). Since the amount of intracellular actin is significantly reduced in *act7* and *act2*, the immunocytochemical approach to observe the effect of 2,4-D or IAA on actin organization was not successful (Figure S6). These results indicate that normal level of actin is required for 2,4-D response in root, and further confirm the link between actin and 2,4-D in root growth response.

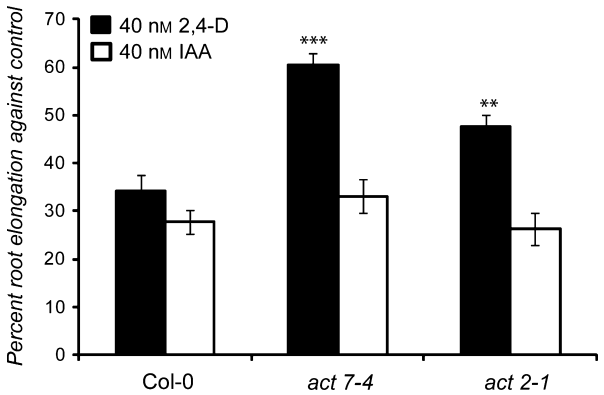

Figure 8. Actin mutants show increased resistance to 2,4-dichlorophenoxyacetic acid (2,4-D)-induced root growth inhibition.
Effect of indole-3-acetic acid (IAA) and 2,4-D on root elongation of *act7-4* and *act8-2*. Five-day-old mutant seedlings were transferred to new agar plates and subjected to 40 nM IAA and 2,4-D treatment for 48 h. Vertical bars represent mean ± SE of the experimental means from at least four independent experiments ($n = 4$ or more), where experimental means were obtained from 8–10 seedlings per experiment. Asterisks represent the statistical significance between control and treatment as judged by the Student's *t*-test ($*^{*}P < 0.001$; $*^{**}P < 0.0001$).

DISCUSSION

The endogenous auxin IAA and its synthetic functional analogue 2,4-D show partially distinct effects in regulating plant developmental processes. 2,4-D-induced inhibition of root growth/plant growth has been shown to be linked to the cellular actin status (Rahman *et al.*, 2007; Rodríguez-Serrano *et al.*, 2014). At a low concentration, 2,4-D but not IAA promotes the depolymerization of root actin and consequently affects the cell division machinery (Figure 3, Table 1; Rahman *et al.*, 2007), while at a herbicidal concentration, 2,4-D promotes the depolymerization of F actin to G actin by affecting the post-translational modification of actin by oxidation and *S*-nitrosylation (Rodríguez-Serrano *et al.*, 2014). These results suggest that 2,4-D and IAA use mechanically distinct pathways to regulate downstream physiological responses. This idea is further reinforced by the isolation of anti-auxin-resistant mutants, which show specific resistance to 2,4-D-induced inhibition of root growth, yet show wild-type sensitivity to IAA (Rahman *et al.*, 2006; Biswas *et al.*, 2007). Using the Arabidopsis root as a model, here we provide cellular and molecular insights into how the 2,4-D–actin interaction modulates root growth. Quantification of actin filaments revealed that the effect of 2,4-D on actin is a rapid and specific process as it alters the cellular actin structure after a short period of incubation. Analyses of different actin parameters further revealed that 2,4-D, but not IAA, reduces the density and the bundling of the actin filaments (Figure 3). Genetic analyses revealed that cellular actin status plays a central role in providing 2,4-D sensitivity in primary root. Both the vegetative class actin mutants *act7-4* and *act2-1* showed increased resistance to 2,4-D but not to IAA-induced inhibition of root growth (Figure 8). Root actin of moderately resistant mutants such as *aar1* and *tir1* shows more susceptibility to 2,4-D-induced changes in structure compared with the mutants that show strong root growth resistance such as *axr1*, aux1 and *aar1tir1*(Figures 4 and 6). These results confirm the involvement of cellular actin in determining the Arabidopsis root growth response to 2,4-D but not to IAA. One potential argument against this conclusion could be the effect of differential intracellular concentrations of 2,4-D and IAA, as IAA is believed to be rapidly

degraded. Several lines of experimental results provide evidence against this argument. In the long-term experiment we found that the IAA and 2,4-D dose response is similar for inhibition of root growth (Figure 5). If IAA is rapidly catabolized then one would expect to see lower potency of IAA in the long-term root growth assay. Similarly, all the auxin-resistant mutants show more sensitivity towards IAA-induced root growth inhibition compared with 2,4-D at the same concentrations, suggesting that IAA degradation is minimal. In the short-term assay, where auxin degradation has been shown to be minimal (Porco *et al.*, 2016), a three-fold increase in IAA concentration did not degrade the actin but rather slightly increased the actin bundling (Figure 3), indicating that 2,4-D and IAA affect the actin structure via distinct mechanisms. One major factor to reduce the degradation of IAA *in vivo* is the light conditions. IAA is more stable under yellow light that filters light below 454 nm to which IAA is labile (Stasinopoulos and Hangarter, 1990). This conditional effect is also reflected in the potency of IAA to inhibit root growth (Rahman *et al.*, 2001b, 2007). The effect of light conditions on IAA metabolism has also been shown in recent studies where two different groups reported different phenotypes of the same *AtDAO1* loss-of-function mutant (Porco *et al.*, 2016; Zhang *et al.*, 2016). *DAO1* has been shown to be the major regulator of IAA oxidation and homeostasis in Arabidopsis (Porco *et al.*, 2016; Zhang *et al.*, 2016). The phenotypic differences observed in two different studies were attributed to the difference in the light intensity used to grow the plants. Lower-intensity light resulted in more basal IAA levels (Zhang *et al.*, 2016). Further, it has also been shown that loss- or gain-of-function *AtDAO1* lines exhibit a subtle phenotype and no changes in intracellular IAA level, indicating that IAA conjugation and catabolism seem to regulate IAA homeostasis in a highly redundant manner (Mellor *et al.*, 2016; Porco *et al.*, 2016; Zhang *et al.*, 2016). Collectively, these results confirm that the observed differential effect of 2,4-D and IAA on the actin cytoskeleton is not due to differences in the intracellular IAA concentration mediated by rapid degradation of IAA.

Identification and characterization of the genes that confer 2,4-D-specific resistance in roots revealed that these gene products are tightly linked to the ubiquitin proteasome pathway. SMAP1, which is deleted in *aar1*, interacts with CSN, and DCN1-like protein, which is mutated in *aar3*, has been speculated to interact with the ubiquitin-like protein Nedd8 (Biswas *et al.*, 2007; Nakasone *et al.*, 2012). Recently a human orthologue of SMAP1 was identified as the ninth subunit of CSN (Rozen *et al.*, 2015). CSN is a key regulator of all cullin-RING ubiquitin ligases, the largest family of E3 ubiquitin ligases including SCF$^{TIR1/AFB}$, which is the major upstream pathway that regulates auxin signaling (reviewed in Gray and Estelle, 2000). All the mutants in this pathway showed resistance to both 2,4-D- and IAA-induced root growth inhibition (Ruegger *et al.*, 1998; reviewed in Leyser, 2001; Hellmann *et al.*, 2003), and this resistance was attributed to alteration in the auxin signaling system. However, the current findings, (i) that blocking the ubiquitin proteasome pathway by a general ubiquitin proteasome inhibitor MG132 resulted in complete resistance to the 2,4-D-induced depolymerization of actin in short-term assay (Figure 7), and (ii) increased resistance of all the SCF^{TIR1} mutants to 2,4-D-induced depolymerization of actin in long-term assay (Figure 6), suggest that in addition to auxin signaling, SCF^{TIR} ubiquitin proteasome pathway also functions in regulating the actin pathway that is sensitive to 2,4-D.

Although SMAP1 functions more in 2,4-D-specific pathways, it also affects the endogenous auxin response under selective conditions. SMAP1 has been shown to be required for normal plant growth and development and the response of root growth to IAA or methyl jasmonate in the *axr1* mutant background (Nakasone *et al.*, 2012). The extreme dwarf phenotype of *aar1-1csn5a-1* further suggests that SMAP1 plays an important role in regulating plant development under limiting CSN functionality, and possibly modulates auxin response and other cullin-RING ubiquitin-ligase related signaling processes via its interaction with components associated with modification of RUB (Nakasone *et al.*, 2012). Consistently, here we observed that the double mutant *aar1-1tir1*-1 showed increased resistance to root growth inhibition induced by low concentrations of IAA compared with the respective single mutants (Figure 5). These results indicate that SMAP1 and ubiquitin pathways are tightly linked and further confirm our previous observation that SMAP1 is a conditional modulator of IAA response.

Actins are important regulators of cell and organ development. One of the actin isovariants *ACT7* has been shown to be an important regulator of primary root development. This isoform has also been shown to be responsive to various hormones, including IAA and 2,4-D. Both IAA and 2,4-D inhibit the expression of *ACT7* in root meristem but stimulate it in the lateral root primordial-like structure (McDowell *et al.*, 1996). Loss of *ACT7* but not *ACT2* results in slower callus formation in callus induction medium (CIM), which contains both 2,4-D and kinetin (Kandasamy *et al.*, 2001). Consistently, the loss of *ACT2* only affects the root hair phenotype of the primary root (Kandasamy *et al.*, 2009; Figure S5). Interestingly, there are no data available for the response of primary root growth in these mutants to 2,4-D or IAA. Considering the differential effect of ACT7 and ACT2 on primary root growth, we expected to observe a differential response to 2,4-D and IAA in these two mutants. In addition, since 2,4-D degrades actin in wild type, and both *act2* and *act7* mutants have extremely reduced amount of actin (Kandasamy *et al.*, 2009; Figure S6), we expected a hypersensitive response of these mutants to 2,4-D. Surprisingly, both *act2-1* and *act7-4*

showed selective resistance to 2,4-D (Figure 8). There are two plausible hypotheses to explain this result. Since 2,4-D partially functions through actin to regulate the root growth, an intact cell cytoskeletal structure is necessary to exert its effect. *act2* and *act7* mutants have a global deficiency in actin which results in a general reduction of the target for 2,4-D, and hence these mutants become resistant to 2,4-D-induced inhibition of root growth. However, there is a clear difference in the extent of resistance to 2,4-D in these mutants. The *act7* mutant showed more resistance to 2,4-D than *act2*, which is consistent with the above hypothesis as *act7* mutants have a much lower amount of actin than *act2* (Kandasamy *et al.*, 2009). Alternatively, this selective difference may be related to the altered distribution of the auxin influx transporter AUX1. Several studies have reported that some but not all the auxin transporters trafficking and localizations are actin dependent (Geldner *et al.*, 2001; Kleine-Vehn *et al.*, 2006; Rahman *et al.*, 2007; Shibasaki *et al.*, 2009; Cho *et al.*, 2012). An intact cytoskeleton is a strict requirement for subcellular trafficking and the polar localization of AUX1. Treatment with Lat B resulted in intracellular agglomeration and mislocalization of AUX1. It was also shown that the targeting of AUX1 is more sensitive to Lat B compared with PIN1 (Kleine-Vehn *et al.*, 2006). Based on these results, one assumption could be that in actin mutants AUX1 localization is disrupted, resulting in lower uptake of 2,4-D and making these mutants resistant to 2,4-D- induced inhibition of root growth. In contrast, uptake of IAA by roots is mediated via lipophilic uptake, AUX1 and the ATP-binding cassette B4 (ABCB4) (Marchant *et al.*, 1999; Rahman *et al.*, 2001a; Kubeš *et al.*, 2012). ABCB4 has been shown to be stably associated with membranes and the trafficking of this protein is less dependent on actin (Cho *et al.*, 2012). In actin mutants, membrane-associated ABCB4 may function to facilitate the carrier-mediated uptake of IAA as well as the lipophilic uptake, resulting in inhibition of root growth.

In conclusion, this work provides molecular and cellular evidence to support the idea that the 2,4-D response pathway in Arabidopsis is tightly linked to actin, and actin filament organization partially dictates the sensitivity of roots to 2,4-D. Components of the SCF^{TIR1} ubiquitin proteasome pathway and a unique protein, SMAP1, which interacts with the ubiquitin component, appear to regulate this pathway. This finding is intriguing, as ubiquitin proteasome regulates the response pathways by degrading proteins, raising the possibility that actin/actin-binding proteins may be subjected to ubiquitin-dependent protein degradation in the presence of 2,4-D. In support of this notion is the observation that light-mediated promotion of root growth in Arabidopsis is facilitated in part through the degradation of the actin regulatory protein SCAR via the proteasome pathway (Dyachok *et al.*, 2011). The biological significance of this pathway is possibly linked to the herbicidal action of 2,4-D. It is interesting to note that all classes of auxinic herbicides (phenoxyalkanoic acids, e.g. 2,4-D; benzoic acids, e.g. dicamba; pyridine carboxylic acids, e.g. picloram) use SCF ubiquitin pathway. For instance, both dicamba and picloram require the SCF^{AFB5} pathway to exert their herbicidal effect on Arabidopsis (Walsh *et al.*, 2006; Gleason *et al.*, 2011). In screening for mutants resistant to picolinate auxin, Walsh *et al.* (2006) also identified *SGT1b* as a target gene for picloram. In yeast, SGT1b physically interacts with a variety of multiprotein complexes, including SCF ubiquitin ligase (Kitagawa *et al.*, 1999). In plants, mutation in *SGT1b* results in enhanced resistance of *tir1-1*to IAA by altering the degradation of AUX/IAA protein, suggesting that SGT1b is required for some elements of SCF function (Gray *et al.*, 2003). An AFB5–TIR1 double mutant showed greater resistance to dicamba, indicating that both SCF^{AFB5} and SCF^{TIR1} may contribute to distinct dicamba responses (Gleason *et al.*, 2011). Consistently, it was demonstrated that *axr1* mutant shows a 160-fold increase in resistance towards picloram over wild-type, while *afb5* mutant shows only a 26-fold increase, indicating that SCF ubiquitin pathway that regulates auxin response plays a major role in determining the herbicidal activity of auxinic herbicides (Walsh *et al.*, 2006). We also found that *aar1tir1* double mutant shows increased resistance to 2,4-D compared with the respective single-mutant lines. Taken together, these results suggest that besides regulating the auxin pathway, auxin-related SCF ubiquitin components also play important roles in regulating the herbicidal activity of auxinic herbicides by modulating some as yet unidentified cellular events. In the present work, we demonstrate that intracellular actin organization is an important factor for 2,4-D response, which is modulated by both SMAP1 and SCF^{TIR1}. This pathway may also be linked to the herbicidal action of auxinic herbicides. Future research aimed at identifying the proteins in the actin response pathway that are subjected to protein degradation through SMAP1–SCF^{TIR1} pathway will greatly facilitate our understanding of the role of actin in determining the herbicidal action of 2,4-D.

EXPERIMENTAL PROCEDURES

Plant materials and growth conditions

All lines are in the Columbia background of *Arabidopsis thaliana* (L.) Heynh. The *axr1-12*, *axr1-3*, *aux1-7* and *tir1-1* mutants were obtained from the Arabidopsis Biological Resource Center (https://abrc.osu.edu/). The *aar1-1*, 520i2C, 520i1G, B/S 1G. B/S 2D, X/B lines were described in Rahman *et al.* (2006). *afb2-1* was a kind gift of Nihal Dharmasiri (Texas State University, San Marcos, TX, USA). *tir1-10* (Salk_090445) was a kind gift from Tetsuya Sakai (Nigata University, Japan). The homozygosity of *tir1-10* was confirmed by segregation analysis of the root growth response to 2,4-D and IAA. For live cell imaging, the transgenic ABD2-GFP (Wang *et al.*, 2004) was used. *act7-4* and *act2-1* were a kind gift from Rich Meagher (University of Georgia, Athens, GA, USA) and are described in Kandasamy *et al.* (2009). The *aux1-7* ABD2-GFP was

described in Rahman *et al.* (2007). The *aar1-1*, *tir1-1*, *aar1-1 tir1-1*, and *axr1-3* mutants were introduced into the ABD2-GFP line by crossing and independent lines homozygous for the mutation and expressing the GFP reporter were identified by screening for fluorescence, 2,4-D resistant phenotype and genotyping. At least three independent lines were tested for the phenotype analysis. Crossing to ABD2-GFP did not cause any significant change in root growth phenotype compared with the parental mutant lines.

Surface-sterilized seeds were placed in round, 9-cm Petri plates on modified Hoagland's medium (Baskin and Wilson, 1997) containing 1% w/v sucrose, 1% w/v agar (Difco Bacto agar, BD Laboratories, http://www.bd.com). Two days after stratification at 4°C in the dark, plates were transferred to a growth chamber (LH-70CCFL-CT, NK Systems, http://www.nksystems.jp/) at 23°C under continuous white light at an irradiance of about 100 μmol m^{-2} s^{-1}.

Yellow light was used when plants were treated with IAA, as it prolongs the lifetime of IAA in growth media (Stasinopoulos and Hangarter, 1990). The seedlings were grown vertically for 5 days. For chemical treatment, 5-day-old seedlings were transferred to new plates supplemented with the respective chemicals, and incubated for 2 days under continuous light at an irradiance of about 100 μmol m^{-2} s^{-1}. To measure root elongation, photographs of the plates were taken 48 h after transfer to chemical plates using a digital camera (Power Shot A 640, Canon, http://global.canon/) and analyzed with image analyzing software Image J (http://rsb.info.nih.gov/ij/).

Chemicals

2,4-D, IAA, 2′-7′-dichlorodihydrofluorescin diacetate (DCF-DA) and Lat B were purchased from Sigma Chemical Co. (http://www.sigmaaldrich.com/) Other chemicals were from Wako Pure Chemical Industries (http://www.wako-chem.co.jp/english/).

Immunocytochemistry

To visualize actin, we used the protocol described earlier in Rahman *et al.* (2007). Five-day-old Arabidopsis seedlings were transferred to new agar plates containing each chemical and incubated at 23°C for 2 days. After the 2-day incubation period, roots were immediately fixed in K-PIPES [potassium-piperazine-N,N′-bis(2-ethanesulfonic acid)] buffer containing 4% (v/v) paraformaldehyde, 1.2% (v/v) glutaraldehyde, 1 mM $CaCl_2$ and 4 mM maleimidobenzoyl-*N*-hydroxy succinimide (MBS) and then rinsed three times for 10 min in PME buffer which consists of 50 mM PIPES, 5 mM ethylene glycol-bis (β-aminoethylether)-*N*,*N*,*N*′,*N*′-tetraacetic acid (EGTA) and 2 mM $MgSO_4$. After that, seedlings were extracted for 60 min in PME buffer with 1% Triton X-100 and digested for 15 min in PBS with 0.0001% (v/v) pectolyase and 0.001% (v/v) pectinase, and rinsed three times for 5 min in PME with 10% glycerol and 0.002% Triton X-100. Next, to permeate cell walls, seedlings were incubated at −20°C in methanol for 30 min, and were rehydrated for 5 min (three times) in PBS. Seedlings were incubated in the mouse monoclonal anti-(chicken gizzard) actin (Anti-Actin, clone C4, Millipore, http://www.millipore.com/), diluted 1:200 in PBS, 1% BSA and 0.01% sodium azide (PBA) overnight. The seedlings were washed for three times in PBS and the secondary antibody, Cy-3-goat anti-mouse IgG (1:200, Jackson Immunoresearch, http://www.jacksonimmuno.com/) was applied.

The imaging was done on an Olympus BX-61 upright microscope (http://www.olympus.com/), equipped with a Yokogawa confocal attachment (https://www.yokogawa.com/), and imaged with a 60 × oil-immersion objective with a numerical aperture of 1.40.

Live cell imaging

Five-day-old GFP-transgenic seedlings were used for live cell microscopy. For 2,4-D, IAA and Lat B treatment, 5-day-old seedlings were incubated in each chemical for 2 days on modified Hoagland medium as described earlier in 'Plant materials and growth conditions'. The concentrations of the hormones and inhibitors are mentioned in the figures. The roots were mounted in liquid modified Hoagland medium on a cover glass and visualized using a Nikon laser scanning microscope (Eclipse T1 equipped with Nikon C2 Si laser scanning unit, http://www.nikon.com/) using a 40 × water immersion objective with a numerical aperture of 1.25.

Actin quantification

A short-term assay was developed for actin quantification. Five-day-old ABD2-GFP seedlings were transferred to a six-well Petri dish containing 3 ml of Hoagland solution. The seedlings were incubated in the presence or absence of 1 μM and 3 μM IAA and 2,4-D for 1 h and subjected to imaging with the Nikon laser scanning microscope using same laser set up. For ubiquitin proteasome inhibitor assay, the roots were pre-treated with 50 μM MG132 for 30 min and then incubated with 3 μM 2,4-D for 1 h. After the incubation, the images were taken as described in 'Live cell imaging'. All the experiments were repeated at least three or four times. Actin quantification was performed using ImageJ software (http://rsb.info.nih.gov/ij/) as described earlier (Higaki *et al.*, 2010). Before measurements of actin parameters, the confocal images were skeletonized with using the ImageJ plug-in KbiLineExtract (Ueda *et al.*, 2010). Using the processed images, we measured four different parameters; occupancy for density, skewness for bundling, $\Delta\theta$ for orientation and NormAvgRad for parallelness. Occupancy was defined as a percentage of skeletonized ABD2-GFP pixel numbers per cell region pixel numbers. This occupancy parameter is decreased by the disruption of actin filaments (Higaki *et al.*, 2010). Skewness of the skeletonized ABD2-GFP intensity distribution is used for actin filament bundling. This skewness becomes higher when ABD2-GFP signal is increased by bundling (Higaki *et al.*, 2010). $\Delta\theta$ indicates the mean angular difference between the mean angle of skeletonized ABD2-GFP line segments and the angle of the major axis of the cell. This $\Delta\theta$ has its maximum value of 90° when skeletonized ABD2-GFP line segments have complete transverse orientation and its lowest value of 0° when the filaments have complete longitudinal orientation. NormAvgRad is a metric parameter for parallelness of the skeletonized ABD2-GFP line segments, and can range from 0 to 1 (Ueda *et al.*, 2010). This parallelness becomes higher as actin filaments run parallel to each other, and becomes lower when actin filaments have a random orientation. All these parameters were measured using the ImageJ plug-in KbiLineFeature (Higaki *et al.*, 2010; Ueda *et al.*, 2010).

Root growth, cell length and cell production rate assays

Seedlings were grown vertically for 5 days after stratification. On day 5, seedlings were transferred to medium with or without chemicals and grown vertically for another 2 days. 2,4-D was dissolved initially in DMSO and diluted into molten agar just prior to gelling. The dilution was 1000-fold and control media received an equivalent volume of DMSO.

Root elongation rate was measured by scoring the position of the root tip on the back of the Petri plate once per day, as described by Baskin and Wilson (1997). Cortical cell length was measured using a light microscope (Diaphot, Nikon) equipped with a digital camera control unit (Digital Sight DS-L2, Nikon). To ensure that

newly matured cells were scored, no cell was measured closer to the tip than the position where root hair length was roughly half maximum. The length of 10 mature cortical cells was measured from each root, with five roots used per treatment. Cell production rate was calculated by taking the ratio of root elongation rate on the third day after transfer and the average cell length for each individual and averaging over all the roots in the treatment. The reported experiments are based on three replicates per treatment; all these experiments have themselves been repeated three times.

Cell clearing

Cell clearing was conducted to stop the growth of seedlings and see clear cortical cell images for measuring cell length. The seedlings were pre-incubated in 0.24 N HCl in 20% methanol at 57°C for 15 min, followed by incubation in 7% NaOH in 60% ethanol for 15 min at room temperature. Seedlings were then rehydrated for 5 min each in 40%, 20% and 10% ethanol. Finally, the roots were incubated in 5% ethanol and 50% glycerol for 15 min. To visualize the cleared cells, the seedlings were mounted in 50% glycerol and observed under a light microscope (Diaphot, Nikon) equipped with a digital camera control unit (Digital Sight DS-L2, Nikon).

Statistical analysis

Results are expressed as the means ± SE from an appropriate number of experiments as described in the figure legends. Two-tailed Student's *t*-test or Tukey–Kramer multiple comparison tests were performed to analyze statistical significance using R (https://www.r-project.org/).

ACCESSION NUMBERS

Sequence data from this article can be found in the Arabidopsis Genome Initiative under the following accession numbers: *AUX1* (At2 g38120), *SMAP1* (At4 g13520), *AXR1* (At1 g05180), *TIR1* (At3 g62980), *AFB2* (At3 g26810), *ACT2* (At3 g18780), *ACT7* (At5 g09810).

ACKNOWLEDGEMENTS

This work was supported in part by JSPS KAKENHI Grant from the Ministry of Culture, Sports, Science and Technology, Japan (grant no. JP19780246 and JP21780305 to AR) and the Oklahoma Center for the Advancement of Science and Technology (OCAST grant no. PS15-012 to EBB). The authors declare no conflict of interest.

AUTHOR CONTRIBUTIONS

AR designed the study; MT and KU carried out the experiments; TH performed the image analyses for actin quantification; YO and EBB provided materials and discussed the study with AR. All authors analyzed and discussed the data. AR, MT and EBB wrote the paper.

SUPPORTING INFORMATION

Additional Supporting Information may be found in the online version of this article.

Figure S1. Comparison of the effect of 2,4-dichlorophenoxyacetic acid and indole-3-acetic acid on root growth inhibition in *tir1-10* and complemented and non-complemented lines of *aar1*.

Figure S2. Comparison of the effect of 2,4-dichlorophenoxyacetic acid and indole-3-acetic acid on root growth inhibition in *afb* mutants.

Figure S3. Auxin signaling mutants are sensitive to latrunculin B.

Figure S4. *Arabidopsis thaliana* actin family.

Figure S5. Effect of 2,4-dichlorophenoxyacetic acid and indole-3-acetic acid on root growth in actin mutants.

Figure S6. Intracellular actin organization of *act7-4* and *act2-1*.

REFERENCES

Baskin, T.I. and Wilson, J.E. (1997) Inhibitors of protein kinases and phosphatases alter root morphology and disorganize cortical microtubules. *Plant Physiol.* **113**, 493–502.

Beemster, G.T. and Baskin, T.I. (1998) Analysis of cell division and elongation underlying the developmental acceleration of root growth in *Arabidopsis thaliana*. *Plant Physiol.* **116**, 1515–1526.

Bennett, M.J., Marchant, A., Green, H.G., May, S.T., Ward, S.P., Millner, P.A., Walker, A.R., Schulz, B. and Feldmann, K.A. (1996) Arabidopsis *AUX1* gene: a permease-like regulator of root gravitropism. *Science*, **273**, 948–950.

Biswas, K.K., Ooura, C., Higuchi, K. *et al.* (2007) Genetic characterization of mutants resistant to the antiauxin *p*-chlorophenoxyisobutyric acid reveals that *AAR3*, a gene encoding a DCN1-like protein, regulates responses to the synthetic auxin 2,4-dichlorophenoxyacetic acid in Arabidopsis roots. *Plant Physiol.* **145**, 773–785.

Brunoud, G., Wells, D.M., Oliva, M. *et al.* (2012) A novel sensor to map auxin response and distribution at high spatio-temporal resolution. *Nature*, **482**, 103–106.

Calderón Villalobos, L.I.A., Lee, S., Oliveira, C.De *et al.* (2012) A combinatorial TIR1/AFB-Aux/IAA co-receptor system for differential sensing of auxin. *Nat. Chem. Biol.* **8**, 477–485.

Campanoni, P. and Nick, P. (2005) Auxin-dependent cell division and cell elongation. 1-Naphthaleneacetic acid and 2,4-dichlorophenoxyacetic acid activate different pathways. *Plant Physiol.* **137**, 939–948.

Carrier, D.J., Bakar, N.T.A., Swarup, R., Callaghan, R., Napier, R.M., Bennett, M.J. and Kerr, I.D. (2008) The binding of auxin to the Arabidopsis auxin influx transporter AUX1. *Plant Physiol.* **148**, 529–535.

Cho, M., Lee, Z.-W. and Cho, H.-T. (2012) ATP-Binding Cassette B4, an auxin-efflux transporter, stably associates with the plasma membrane and shows distinctive intracellular trafficking from that of PIN-FORMED proteins. *Plant Physiol.* **159**, 642–654.

Coué, M., Brenner, S.L., Spector, I. and Korn, E.D. (1987) Inhibition of actin polymerization by latrunculin A. *FEBS Lett.* **213**, 316–318.

Delbarre, A., Muller, P., Imhoff, V. and Guern, J. (1996) Comparison of mechanisms controlling uptake and accumulation of 2,4-dichlorophenoxy acetic acid, naphthalene-1-acetic acid, and indole-3-acetic acid in suspension-cultured tobacco cells. *Planta*, **198**, 532–541.

Dharmasiri, N., Dharmasiri, S., Weijers, D., Lechner, E., Yamada, M., Hobbie, L., Ehrismann, J.S., Jürgens, G. and Estelle, M. (2005) Plant development is regulated by a family of auxin receptor F box proteins. *Dev. Cell*, **9**, 109–119.

Dyachok, J., Zhu, L., Liao, F., He, J., Huq, E. and Blancaflor, E.B. (2011) SCAR mediates light-Induced root elongation in *Arabidopsis* through photoreceptors and proteasomes. *Plant Cell*, **23**, 3610–3626.

Estelle, M.A. and Somerville, C. (1987) Auxin-resistant mutants of *Arabidopsis thaliana* with an altered morphology. *Mol. Gen. Genet.* **206**, 200–206.

Geldner, N., Friml, J., Stierhof, Y.D., Jurgens, G. and Palme, K. (2001) Auxin transport inhibitors block PIN1 cycling and vesicle trafficking. *Nature*, **413**, 425–428.

Gilliland, L.U., Kandasamy, M.K., Pawloski, L.C. and Meagher, R.B. (2002) Both vegetative and reproductive actin isovariants complement the stunted root hair phenotype of the Arabidopsis *act2-1* mutation. *Plant Physiol.* **130**, 2199–2209.

Gilliland, L.U., Pawloski, L.C., Kandasamy, M.K. and Meagher, R.B. (2003) *Arabidopsis* actin gene *ACT7* plays an essential role in germination and root growth. *Plant J.* **33**, 319–328.

Gleason, C., Foley, R.C. and Singh, K.B. (2011) Mutant analysis in Arabidopsis provides insight into the molecular mode of action of the auxinic herbicide dicamba. *PLoS ONE*, **6**. doi:10.1371/journal.pone.0017245.

Gray, W.M. and Estelle, M. (2000) Function of the ubiquitin-proteasome pathway in auxin response. *Trends Biochem. Sci.* **25**, 133–138.

Gray, W.M., Kepinski, S., Rouse, D., Leyser, O. and Estelle, M. (2001) Auxin regulates SCF(TIR1)-dependent degradation of AUX/IAA proteins. *Nature*, **414**, 271–276.

Gray, W.M., Muskett, P.R., Chuang, H.-W. and Parker, J.E. (2003) Arabidopsis SGT1b is required for SCF ^{TIR1} -mediated auxin response. *Plant Cell*, **15**, 1310–1319.

Hayashi, K.I., Jones, A.M., Ogino, K., Yamazoe, A., Oono, Y., Inoguchi, M., Kondo, H. and Nozaki, H. (2003) Yokonolide B, a novel inhibitor of auxin action, blocks degradation of AUX/IAA factors. *J. Biol. Chem.* **278**, 23797–23806.

Hellmann, H., Hobbie, L., Chapman, A., Dharmasiri, S., Dharmasiri, N., Pozo, C.Del, Reinhardt, D. and Estelle, M. (2003) Arabidopsis *AXR6* encodes CUL1 implicating SCF E3 ligases in auxin regulation of embryogenesis. *EMBO J.* **22**, 3314–3325.

Higaki, T., Kutsuna, N., Sano, T., Kondo, N. and Hasezawa, S. (2010) Quantification and cluster analysis of actin cytoskeletal structures in plant cells: role of actin bundling in stomatal movement during diurnal cycles in Arabidopsis guard cells. *Plant J.* **61**, 156–165.

Jackson, R.G., Kowalczyk, M., Li, Y., Higgins, G., Ross, J., Sandberg, G. and Bowles, D.J. (2002) Over-expression of an Arabidopsis gene encoding a glucosyltransferase of indole-3-acetic acid: phenotypic characterisation of transgenic lines. *Plant J.* **32**, 573–583.

Kandasamy, M.K., Gilliland, L.U., McKinney, E.C. and Meagher, R.B. (2001) One plant actin isovariant, *ACT7*, is induced by auxin and required for normal callus formation. *Plant Cell*, **13**, 1541–1554.

Kandasamy, M.K., McKinney, E.C. and Meagher, R.B. (2009) A single vegetative actin isovariant overexpressed under the control of multiple regulatory sequences is sufficient for normal *Arabidopsis* development. *Plant Cell*, **21**, 701–718.

Kepinski, S. and Leyser, O. (2005) The Arabidopsis F-box protein TIR1 is an auxin receptor. *Nature*, **435**, 446–451.

Khurana, P., Henty, J.L., Huang, S., Staiger, A.M., Blanchoin, L. and Staiger, C.J. (2010) Arabidopsis VILLIN1 and VILLIN3 have overlapping and distinct activities in actin bundle formation and turnover. *Plant Cell*, **22**, 2727–2748.

Kitagawa, K., Skowyra, D., Elledge, S.J., Harper, J.W. and Hieter, P. (1999) SGT1 encodes an essential component of the yeast kinetochore assembly pathway and a novel subunit of the SCF ubiquitin ligase complex. *Mol. Cell*, **4**, 21–33.

Kleine-Vehn, J., Dhonukshe, P., Swarup, R., Bennett, M. and Friml, J. (2006) Subcellular trafficking of the *Arabidopsis* auxin influx carrier AUX1 uses a novel pathway distinct from PIN1. *Plant Cell*, **18**, 3171–3181.

Kubeš, M., Yang, H., Richter, G.L. *et al.* (2012) The Arabidopsis concentration-dependent influx/efflux transporter ABCB4 regulates cellular auxin levels in the root epidermis. *Plant J.* **69**, 640–654.

Leyser, O. (2001) Auxin signalling: the beginning, the middle and the end. *Curr. Opin. Plant Biol.* **4**, 382–386.

Leyser, O. (2002) Molecular genetics of auxin signaling. *Annu. Rev. Plant Biol.* **53**, 377–398.

Leyser, H.M., Lincoln, C.A., Timpte, C., Lammer, D., Turner, J. and Estelle, M. (1993) Arabidopsis auxin-resistance gene *AXR1* encodes a protein related to ubiquitin-activating enzyme E1. *Nature*, **364**, 161–164.

Lincoln, C., Britton, J.H. and Estelle, M. (1990) Growth and development of the *axr1* mutants of Arabidopsis. *Plant Cell*, **2**, 1071–1080.

Maher, E.P. and Martindale, S.J. (1980) Mutants of *Arabidopsis thaliana* with altered responses to auxins and gravity. *Biochem. Genet.* **18**, 1041–1053.

Marchant, A., Kargul, J., May, S.T., Muller, P., Delbarre, A., Perrot-Rechenmann, C. and Bennett, M.J. (1999) AUX1 regulates root gravitropism in Arabidopsis by facilitating auxin uptake within root apical tissues. *EMBO J.* **18**, 2066–2073.

McDowell, J.M., An, Y.Q., Huang, S., McKinney, E.C. and Meagher, R.B. (1996) The Arabidopsis ACT7 actin gene is expressed in rapidly developing tissues and responds to several external stimuli. *Plant Physiol.* **111**, 699–711.

Mellor, N., Band, R. L., Pěnčik, A. *et al.* (2016) Dynamic regulation of auxin oxidase and conjugating enzymes *AtDAO1* and *GH3* modulates auxin homeostasis. *Proc. Natl. Acad. Sci. U. S. A.* **113**, 11022–11027.

Mockaitis, K. and Estelle, M. (2008) Auxin receptors and plant development: a new signaling paradigm. *Annu. Rev. Cell Dev. Biol.* **24**, 55–80.

Nakasone, A., Fujiwara, M., Fukao, Y., Biswas, K.K., Rahman, A., Kawai-Yamada, M., Narumi, I., Uchimiya, H. and Oono, Y. (2012) SMALL ACIDIC PROTEIN1 acts with RUB modification components, the COP9 signalosome, and AXR1 to regulate growth and development of Arabidopsis. *Plant Physiol.* **160**, 93–105.

Parry, G., Calderon-Villalobos, L.I., Prigge, M. *et al.* (2009) Complex regulation of the TIR1/AFB family of auxin receptors. *Proc. Natl. Acad. Sci. U. S. A.* **106**, 22540–22545.

Porco, S., Pěnčik, A., Rashed, A. *et al.* (2016) Dioxygeanse-encoding AtDAO1 gene controls IAA oxidation and homeostasis in *Arabidopsis*. *Proc. Natl. Acad. Sci. U. S. A.* **113**, 10742–10744.

del Pozo, J.C. and Estelle, M. (1999) The Arabidopsis cullin AtCUL1 is modified by the ubiquitin-related protein RUB1. *Proc. Natl. Acad. Sci. U. S. A.* **96**, 15342–15347.

Rahman, A., Ahamed, A., Amakawa, T., Goto, N. and Tsurumi, S. (2001a) Chromosaponin I specifically interacts with AUX1 protein in regulating the gravitropic response of Arabidopsis roots. *Plant Physiol.* **125**, 990–1000.

Rahman, A., Amakawa, T., Goto, N. and Tsurumi, S. (2001b) Auxin is a positive regulator for ethylene-mediated response in the growth of Arabidopsis Roots. *Plant Cell Physiol.* **42**, 301–307.

Rahman, A., Nakasone, A., Chhun, T. *et al.* (2006) A small acidic protein 1 (SMAP1) mediates responses of the Arabidopsis root to the synthetic auxin 2,4-dichlorophenoxyacetic acid. *Plant J.* **47**, 788–801.

Rahman, A., Bannigan, A., Sulaman, W., Pechter, P., Blancaflor, E.B. and Baskin, T.I. (2007) Auxin, actin and growth of the *Arabidopsis thaliana* primary root. *Plant J.* **50**, 514–528.

Rodríguez-Serrano, M., Pazmiño, D.M., Sparkes, I., Rochetti, A, Hawes, C., Romero-Puertas, M.C. and Sandalio, L.M. (2014) 2,4-Dichlorophenoxyacetic acid promotes S-nitrosylation and oxidation of actin affecting cytoskeleton and peroxisomal dynamics. *J. Exp. Bot.* **65**, 4783–4793.

Rozen, S., Füzesi-Levi, M.G., Ben-Nissan, G., Mizrachi, L., Gabashvili, A., Levin, Y., Ben-Dor, S., Eisenstein, M. and Sharon, M. (2015) CSNAP is a stoichiometric subunit of the COP9 signalosome. *Cell Rep.* **13**, 585–598.

Ruegger, M., Dewey, E., Gray, W.M., Hobbie, L., Turner, J. and Estelle, M. (1998) The TIR1 protein of Arabidopsis functions in auxin response and is related to human SKP2 and yeast Grr1p. *Genes Dev.* **12**, 198–207.

Rybel, B.De, Audenaert, D., Beeckman, T. and Kepinski, S. (2009) The past, present, and future of chemical biology in auxin research. *ACS Chem. Biol.* **4**, 987–998.

Shibasaki, K., Uemura, M., Tsurumi, S. and Rahman, A. (2009) Auxin response in Arabidopsis under cold Stress: underlying molecular mechanisms. *Plant Cell*, **21**, 3823–3838.

Silk, W.K., Lord, E.M. and Eckard, K.J. (1989) Growth patterns inferred from anatomical records : empirical tests using longisections of roots of Zea mays L. *Plant Physiol.* **90**, 708–713.

Spector, I., Shochet, N.R., Kashman, Y. and Groweiss, A. (1983) Latrunculins: novel marine toxins that disrupt microfilament organization in cultured cells. *Science*, **219**, 493–495.

Spector, I., Shochet, N.R., Blasberger, D. and Kashman, Y. (1989) Latrunculins-novel marine macrolides that disrupt microfilament organization and affect cell growth: I. Comparison with cytochalasin D. *Cell Motil. Cytoskeleton*, **13**, 127–144.

Stasinopoulos, T.C. and Hangarter, R.P. (1990) Preventing photochemistry in culture media by long-pass light filters alters growth of cultured tissues. *Plant Physiol.* **93**, 1365–1369.

Staswick, P.E., Serban, B., Rowe, M., Tiryaki, I., Maldonado, M.T., Maldonado, M.C. and Suza, W. (2005) Characterization of an Arabidopsis enzyme family that conjugates amino acids to indole-3-acetic acid. *Plant Cell*, **17**, 616–627.

Ueda, H., Yokota, E., Kutsuna, N., Shimada, T., Tamura, K., Shimmen, T., Hasezawa, S., Dolja, V.V. and Hara-Nishimura, I. (2010) Myosin-dependent endoplasmic reticulum motility and F-actin organization in plant cells. *Proc. Natl. Acad. Sci. U. S. A.* **107**, 6894–6899.

Walsh, T.A., Neal, R., Merlo, A.O., Honma, M., Hicks, G.R., Wolff, K., Matsumura, W. and Davies, J.P. (2006) Mutations in an auxin receptor homolog AFB5 and in SGT1b confer resistance to synthetic picolinate auxins and not to 2,4-dichlorophenoxyacetic acid or indole-3-acetic acid in Arabidopsis. *Plant Physiol.* **142**, 542–552.

Wang, Y.S., Motes, C.M., Mohamalawari, D.R. and Blancaflor, E.B. (2004) Green fluorescent protein fusions to Arabidopsis Fimbrin 1 for spatio-

temporal imaging of F-actin dynamics in roots. *Cell Motil. Cytoskeleton*, **59**, 79–93.

Yamamoto, M. and Yamamoto, K.T. (1998) Differential effects of 1-naphthaleneacetic acid, indole-3-acetic acid and 2,4-dichlorophenoxyacetic acid on the gravitropic response of roots in an auxin-resistant mutant of arabidopsis, *aux1*. *Plant Cell Physiol.* **39**, 660–664.

Zhang, J., Jinshan, E. L., Harris, C., Pereira, M. C. F., Wu, F., Blakeslee, J. J. and Peer, W. A. (2016) DAO1 catalyzes temporal and tissue-specific oxidative inactivation of auxin in *Arabidopsis thalaiana*. *Proc. Natl. Acad. Sci. U. S. A.* **113**, 11010–11015.